

**NJC****Hydrogen generation and degradation of trypan blue by
Fern-like structured Silver doped TiO₂ nanoparticles**

Journal:	<i>New Journal of Chemistry</i>
Manuscript ID:	NJ-ART-08-2014-001403.R1
Article Type:	Paper
Date Submitted by the Author:	24-Nov-2014
Complete List of Authors:	Ganganagappa, Nagaraju; UFRGS, Chemistry Ravishankar, Thammadihalli; Jain University, Centre for Nano and Material Sciences Ramakrishnappa, Thippeswamy; Jain University, Centre for Nano and Material Sciences H, Nagabhushana; Tumkur University, deSouza, Virginia; UFRGS, Institute of Chemistry Dupont, Jairton; Institute of Chemistry, Laboratory of Molecular Catalysis

SCHOLARONE™
Manuscripts

Hydrogen generation and degradation of trypan blue by Fern-like structured Silver doped TiO₂ nanoparticles

Thammadihalli Nanjundaiah Ravishankar¹, Thippeswamy Ramakrishnappa^{1*}, Hanumanthappa Nagabhushana², Virginia deSouza³, Jairton Dupont³ and Ganganagappa Nagaraju^{1,4*},

¹Centre for Nano and Material Sciences, Jain University, Jakkasandra, Kanakapura (T), India

²CNR Rao Center for Advanced Materials, Tumkur University, Tumkur, India

³Laboratory of Molecular Catalysis, Institute of Chemistry, UFRGS, Porto Alegre, Brasil

⁴Departement of Chemistry, Siddaganga Institute of Technology, Tumkur, Karnataka, India

Abstract

TiO₂:Ag nanoparticles have been successfully prepared at 120 °C for one day via ionic liquid assisted hydrothermal method using methoxy ethyl methyl imidazolium methane sulfonate as ionic liquid. The obtained product has been characterized by various techniques. The XRD pattern indicated the formation of TiO₂:Ag nanoparticles, average crystallite size was found to be 40 nm. XPS confirmed that the formation of TiO₂:Ag nanoparticles. UV-Vis spectrum indicated the maximum absorbance at 362 nm which is red shifted compare to nano- sized TiO₂. Surface morphology was analyzed using SEM, which shows leaf like structure of TiO₂:Ag nanoparticles. TEM images showed almost elliptical (rice pellet) shaped nanoparticles with average particle size of about 60 nm. EDS spectrum revealed the presence Ti, O and Ag with atomic percentage 42.6, 43.7 and 2.3% respectively. TiO₂:Ag nanoparticles generate 2230 μmol H₂ per 1 g of photocatalyst at 2.5 h via water splitting reaction at. It also shows good photocatalytic activity in the degradation of trypan blue.

Key words: Nanoparticles, Ionic liquid, Trypan blue, H₂ generation

*Corresponding authors: E-mail: nagarajugn@rediffmail.com (Dr. G. Nagaraju)

ramakrishnappa77@gmail.com (Dr. T. Ramakrishnappa)

1. Introduction

Nanocrystalline transition metal oxides have wide attention due to their unique properties than the bulk metal oxides which are technologically very useful in nano-device fabrications¹⁻². Amongst these metal oxides, TiO₂ nanoparticles are very interesting due to their semiconducting property, wide band gap, low-cost, non-toxic, good oxidizing power and unique properties like promising photocatalyst, sensors and solar cells³. Literature surveys suggested that TiO₂ has some practical limitations, like being efficient in near UV irradiation (4% in the solar spectrum) for effective photocatalysis and recombination of electron-hole pair is very high in bare TiO₂ nanoparticles than the doped TiO₂ nanoparticles. Hence, bare TiO₂ exhibited less photocatalytic activity than the doped TiO₂ nanoparticles⁴. In order to enhance the photocatalytic activity, scientists are working on the synthesis of doped TiO₂ nanoparticles using various methods like hydrothermal, ionic liquid assisted hydrothermal, sol-gel, co-precipitation, combustion and so on⁵. Amongst these methods, ionic liquid assisted hydrothermal is considered as the most prominent, as room temperature ionic liquids (RTILs) has received extensive attention for both academic research and industrial investigations over the past two decades. RTILs possess unique properties such as negligible vapor pressure, wide liquid temperature range, high thermal stability, dissolves both organic and inorganic compounds, high ionic conductivity and wide electrochemical window. An important aspect of the interaction of RTILs with nanoparticle precursors involves the nucleation and growth of nanoparticles⁶. Metal dopants like Ag, Al, Ce, Nd, Eu, Mo, Fe as well as non metal dopants like O, N, S, are used to enhance the photocatalytic activity of TiO₂ nanoparticles⁷. Ag is one of the most promising dopant which brings in surface modification and fabrication of TiO₂ by decreasing the total volume of the particle which in turn, decreases the recombination probability making more carriers available for the oxidation or

reduction on surface⁸. These properties make Ag doped TiO₂ nanoparticles to show enhanced photocatalytic activity (H₂ generation via water splitting reaction and degradation of organic dyes) compare to undoped TiO₂ nanoparticles.

In the 21st century, environmental issues gain prominence because of population explosion and rapid urbanization resulting in energy crisis. Hence researchers are trying to find new alternative routes to prepare energy-generating sources by different methods⁹⁻¹⁰. Amongst various energy sources, H₂ produced by water splitting is an eco-friendly and a highly efficient fuel. Photocatalysis has been considered to be a promising technique for solving energy and environmental issues using abundant sun light¹¹. A significant progress has been achieved on semiconductor based photocatalytic H₂ generation through water splitting over the past several decades, and many excellent reviews have been published¹²⁻¹³. Literature survey says that Ag doped TiO₂ nanoparticles shows enhanced hydrogen generation via water splitting reaction compare to bare TiO₂ nanoparticles¹⁴⁻¹⁵.

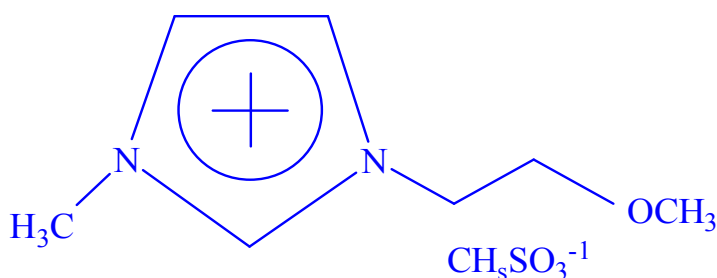
Trypan blue has been used extensively in textile, food and paints industries for dyeing nylon, wool, cotton, silk and also for coloring of oil, fats, waxes, varnish, plastics, etc. Dyes create several environmental problems by releasing highly carcinogenic molecules into the aqueous medium. Hence it is necessary to degrade/remove the industrial effluents containing trypan blue to non-hazardous substances. In this direction, many articles are available on the enhanced photocatalytic activity of Ag doped TiO₂ nanoparticles for the degradation of organic dyes¹⁶⁻¹⁷.

In the present research work, we have used methoxy ethyl methyl imidazolium methane sulfonate (MOEMIMS) as the reaction medium for the synthesis of TiO₂:Ag nanoparticles. These nanoparticles are used as photocatalyst for H₂ generation via water splitting reaction and also in the degradation of trypan blue dye.

2. Experimental

2.1. Preparation of Ionic liquid- Methoxy ethyl methyl imidazolium methane sulfonate (MOEMIMS)

The above ionic liquid was prepared using earlier report¹⁸. 2-methoxyethyl methane sulfonate (5.38 g, 32.0 mmol) was mixed with 1-methyl imidazole (2.62 g, 32.0 mmol) and the reaction mixture was heated to 60 °C for 30 h. The resulting liquid was washed twice with ethyl acetate (5 mL) and dried under vacuum, 1-(2-methoxyethyl)-3-methylimidazolium ethane sulfonate was obtained as colorless and hygroscopic liquid. This IL (MOEMIMS) is used for the preparation of TiO₂:Ag nanoparticles and the structure is as shown in the Scheme.1.



Scheme 1. Structure of 2- Methoxy ethyl methyl imidazolium methane sulfonate.

2.2. Preparation of TiO₂:Ag nanoparticles

0.5 mL TiCl₄ was added to the beaker containing 12 mg silver nitrate and 10 mL MOEMIMS under constant stirring for homogenization. After 5 min, 1 mL water was added to hydrolyze TiCl₄. The white precipitate transferred in to Teflon tube, heat at 120 °C for one day. When the reaction/duration was completed, autoclave was cooled to room temperature naturally. The obtained product was mixed with acetonitrile and stirred for overnight to remove the ionic liquid. Finally TiO₂:Ag nanoparticles were retrieved from centrifugation. The final product was calcined at 400 °C for 3 h.

2.3. Characterization

Powder X-ray diffraction data was recorded on Philips X'pert PRO X-ray diffractometer with graphite monochromatized Cu-K α (1.5418 Å) radiation operated at 40 KV and 30 mA. X-ray photoelectron spectroscopy (XPS) analysis was carried out on an ESCALAB 250 (Thermo-VG Scientific), using Al K α as the excitation source. The instrument was standardized against the C_{1s} spectral line at 284.6 eV. The Fourier transform infrared spectra (FTIR) of the samples were collected using Bruker Alpha-P spectrometer. The absorption spectra of the samples were measured by dispersing the nanoparticles in water and measured using Perkin Elmer Lambda-750 UV-Vis spectrometer. The morphology was examined using table top Hitachi 3000 scanning electron microscopy (SEM). The nanostructure of the product was observed by transmission electron microscopy (TEM) which was performed with JEOL JEM 1200 Ex operating at 100 kV. Samples for TEM were prepared by dropping the dispersion of 2-propanol metal oxide nanoparticle on a holey carbon grid and drying the grids under vacuum for 24 h. The water/organic content present in the sample was investigated by thermo gravimetric analysis (TGA) using a SDT Q600 V20.9 thermo microbalance in N₂ atmosphere from room temperature to 800 °C at a heating rate of 10 °C min⁻¹.

2.4. Photocatalytic H₂ production setup

Photocatalytic H₂ production reaction was carried out in a closed gas-circulating system. TiO₂:Ag nanoparticles were suspended in aqueous ethanol solution by sonicating for about 20 min within an inner irradiation-type reactor made of Pyrex glass. A 240 W Hg–Xe arc lamp (Cermax) was used as excitation source. Prior to the reaction, the mixture was deaerated by purging with Ar gas repeatedly to minimize the oxygen content. The liberated H₂ was periodically analyzed using Agilent 6820 GC Chromatograph equipped with a thermal

conductivity detector and a 5°A molecular sieve packed column with argon as the carrier gas. Using a gas tight syringe with a maximum volume of 50 μL , the amount of H_2 produced was measured at 0.5 h interval of time. The amount of gas liberated is plotted as a function of UV exposure time. During the entire experiment the reaction temperature was kept at 25 °C by eliminating the IR radiation with the circulation of water in the water jacket of the reactor.

2.5. Photocatalytic degradation of Trypan blue

Photocatalytic experiments were carried out in a 150X75 mm batch reactor in the month of November – December at 11-14 h under sun light ($\sim 750 \text{ Wm}^{-2}$ intensity) in Bangalore, India and under UV-light (Mercury lamp as radiation source with 125 Wm^{-2} intensity). An aqueous suspension was prepared by adding known quantity (0.1-0.5 g) of $\text{TiO}_2\text{:Ag}$ nanoparticles to 100 mL trypan blue dye solution at appropriate concentrations (5-25 $\mu\text{g/L}$). For reactions in different pH media, the initial pH was adjusted by the addition of either 0.05 M NaOH or 0.05M H_2SO_4 . During the photocatalytic experiments the slurry composed of dye solution and catalyst was taken in reactor and placed on a magnetic stirrer at a distance 8-10 cm from the light and stirred magnetically at 400 rpm for uniform distribution with simultaneous exposure to UV light/sunlight. Known volume (5 mL) of the exposed solution was withdrawn at specific intervals of time (15 min). $\text{TiO}_2\text{:Ag}$ nanoparticles were removed from the solution by centrifugation to assess the extent of degradation. The dye concentration was measured using a spectrophotometer at 592 nm; various parameters like effect of concentration of the nanoparticles on dye, catalytic load, irradiation time, pH, different light sources, etc. were studied to know the effect on the rate of photo degradation of dye.

3. Results and discussion

3.1. Characterization of the prepared TiO₂:Ag nanoparticles

XRD is mainly used to know the phase composition and crystallite size of the prepared materials.

Fig.1 shows the XRD pattern of the pure TiO₂ and TiO₂:Ag nanoparticles prepared at 120 °C for 1 day via ionic liquid assisted hydrothermal method. The most intense diffraction peak at $2\theta = 25.3^\circ$ confirms the anatase phase TiO₂ (**Fig.1(b)**) and all other diffraction peaks also revealed tetragonal anatase phase TiO₂ nanoparticles with lattice parameters $a = 3.775 \text{ \AA}$, $b = 9.490 \text{ \AA}$ and space group = 141/amd (JCPDS No. 2-387). The two peaks at 44.2° and 64.2° indicate the presence of Ag particles (JCPDS No. 1-1167). The average crystallite size (**Fig.1(b)**) calculated using Debye-Scherer equation for most intense diffraction peak $2\theta = 25.3^\circ$ was found to be 40 nm. **Fig.1 (a)** shows the XRD pattern of tetragonal anatase phase TiO₂ nanoparticles prepared at 120 °C for 1 day via ionic liquid assisted hydrothermal method.

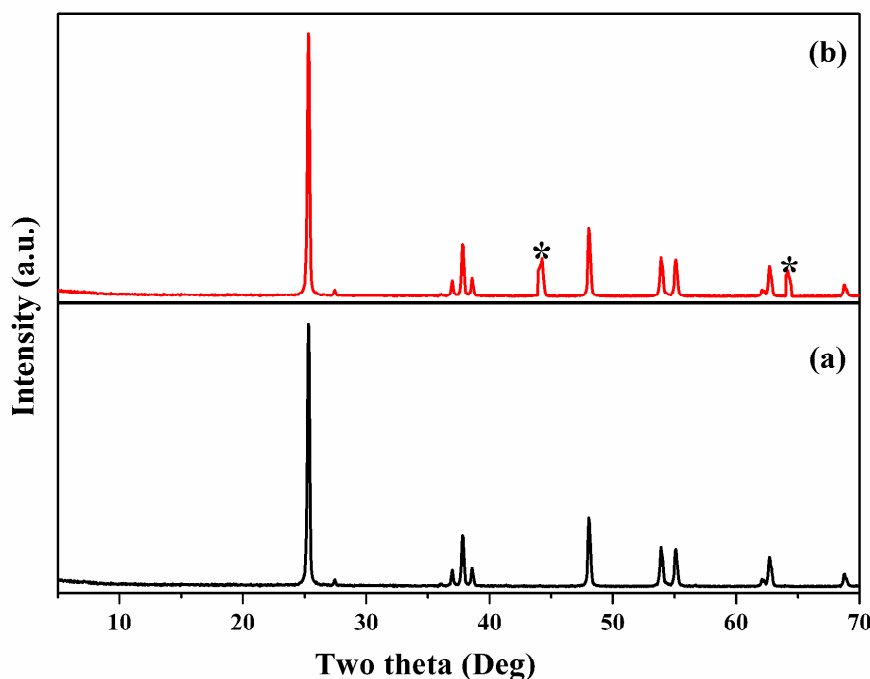


Figure 1. XRD pattern of (a) TiO₂ and (b) TiO₂:Ag nanoparticles (* = Ag)

XPS studies help to find the chemical composition of prepared metal oxide nanomaterial. XPS spectra of $\text{TiO}_2\text{:Ag}$ nanoparticles prepared at $120\text{ }^\circ\text{C}$ for 1 day ionic liquid assisted hydrothermal method was shown in **Fig. 2**. **Fig. 2(a)** shows the XPS spectrum of Ti2p, it is a doublet with the $\text{Ti } 2p_{3/2}$ at 458.5 eV and $\text{Ti}2p_{1/2}$ at 461.67 eV. **Fig. 2(b)** shows the XPS spectrum of O1s, it shows three components centered at 530.1, 533 and 535.2 eV¹⁹. **Fig. 2(c)** represents the XPS spectrum of Ag3d core levels.

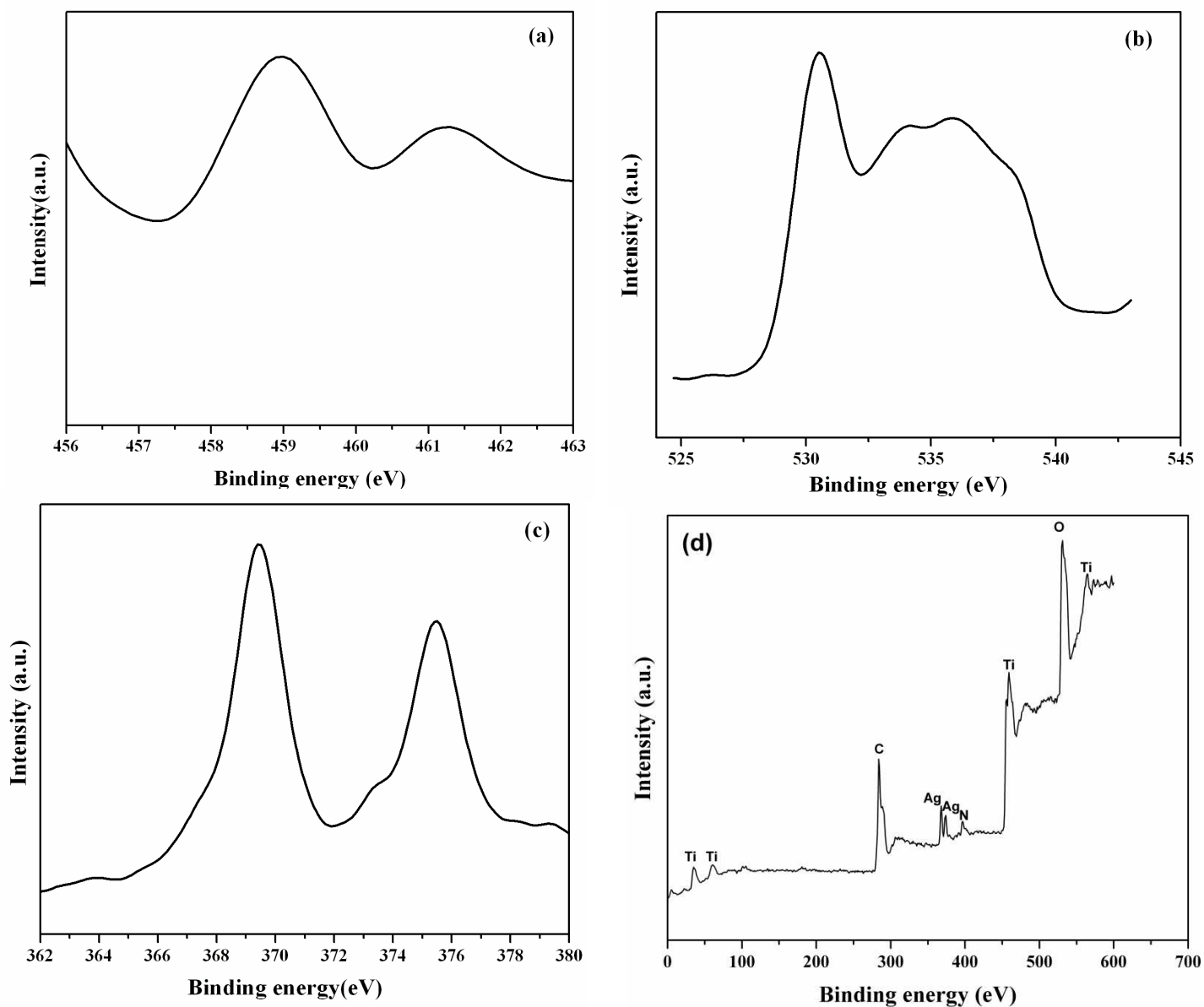


Figure 2. XPS spectra of (a) Ti, (b) O, (c) Ag and (d) wide $\text{TiO}_2\text{:Ag}$ nanoparticles.

The Ag3d_{5/2} and Ag3d_{3/2} core level binding energies appeared at 369 eV and at 375 eV respectively. This is in good agreement with metallic silver reported²⁰. **Fig. 2(d)** shows the broad XPS spectrum of TiO₂:Ag nanoparticles and it shows characteristic peaks of Ti, O and Ag. In addition to these we have also observed the presence of C1s (284.5 eV) and N1s (398.5 eV) suggesting the presence of amino groups. It indicates that, small amount of ionic liquid is still present even after calcination²¹.

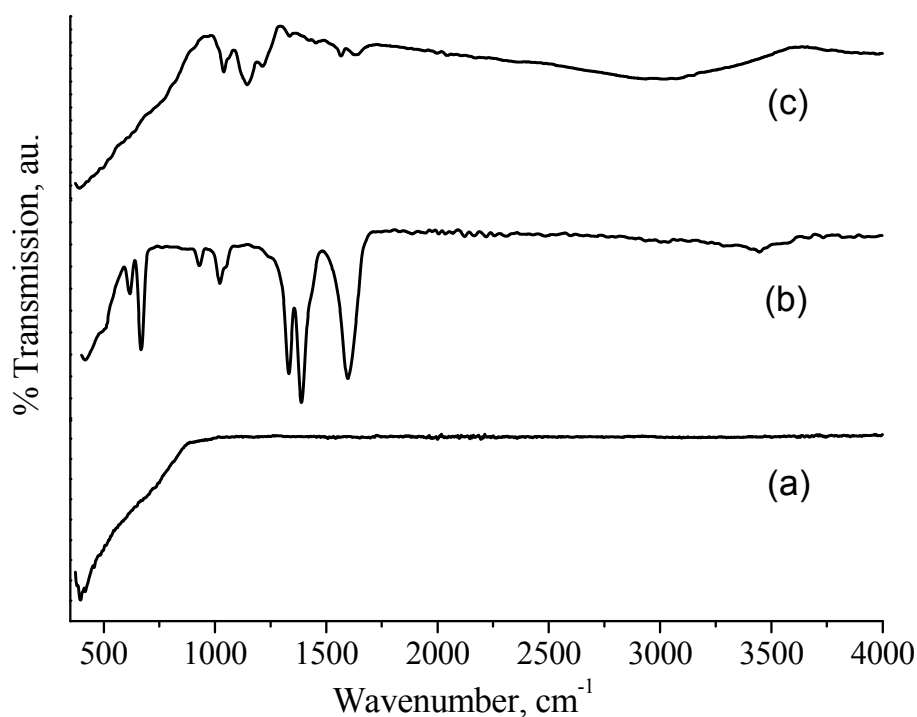


Figure 3. FT-IR spectrum of (a) P25, (b) TiO₂, nanoparticles and (c) TiO₂:Ag nanoparticles.

FT-IR spectroscopy is mainly used to know the presence of functionalized groups present in the synthesized nanomaterials. FTIR spectrum of P25 shows the peak at around 400 cm⁻¹ indicates the characteristic vibrational mode of Ti-O. Pure TiO₂ nanoparticles (**Fig.3 (b)**) also shows a significant peak at around 400 cm⁻¹ due to stretching vibration mode of Ti-O and spectral region

from 1000 to 1700 cm^{-1} can be assigned to C-H, C-C, C=C and N-H stretching/bending vibrations due to the presence of ionic liquid²²⁻²⁴ and it is in good agreement with XPS studies as discussed earlier. FT-IR spectrum of $\text{TiO}_2\text{:Ag}$ nanoparticles (**Fig.3 (c)**) shows various vibrational modes of Ag-O²⁵⁻²⁶ at 500-680 cm^{-1} in addition to characteristics stretching vibration modes of Ti-O peaks at around 415 cm^{-1} .

UV-Vis spectroscopy was used to evaluate the optical properties of the prepared materials. In general, nanomaterials show blue shift compare to bulk, due quantum confinement effect or reduction in the size of the materials. UV Vis spectrum (Figure 4) was taken by sonicating doped/undoped TiO_2 nanomaterials in water for about 20 min. P25 shows broad absorption peak at 400 nm (Figure 4a). TiO_2 nanoparticles (Figure 4b) show an absorption peak at 335 nm which is blue shifted compare to bulk may be due to size effect. $\text{TiO}_2\text{:Ag}$ nanoparticles shows an

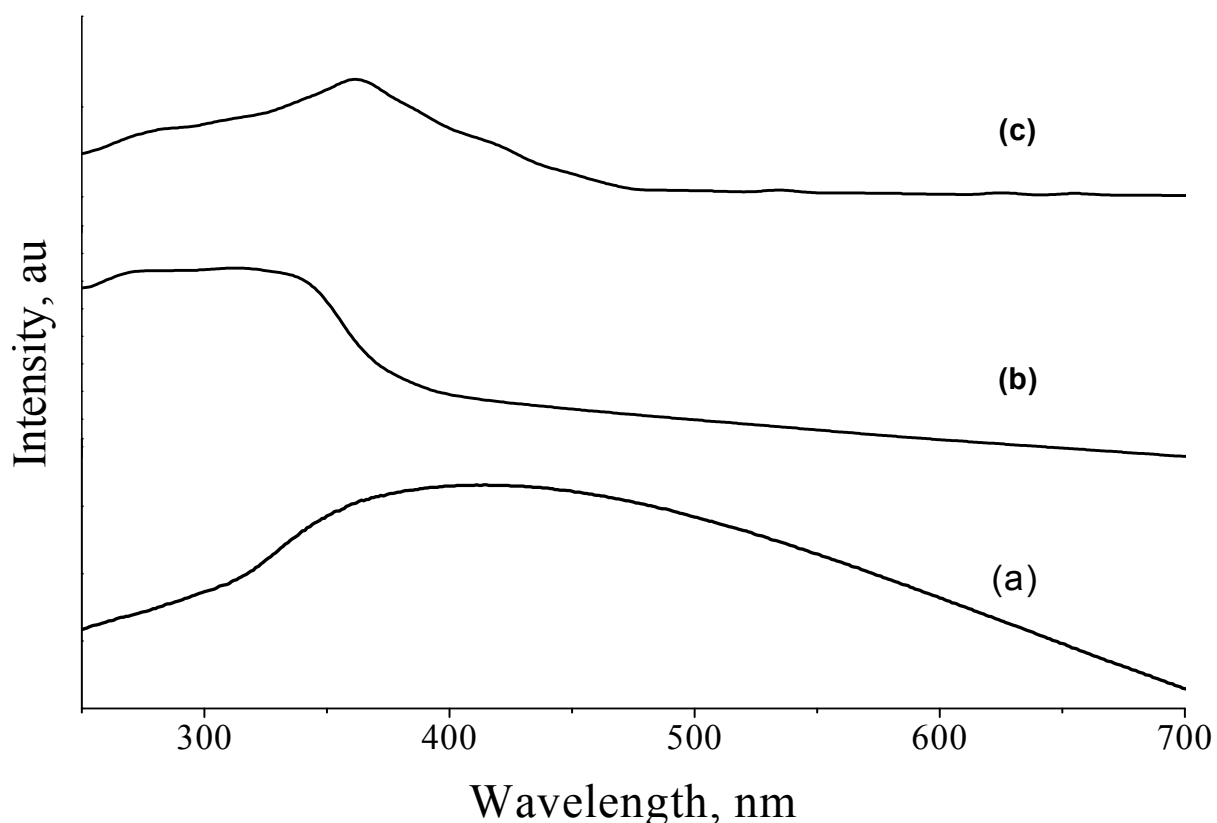


Figure 4. UV-Visible spectrum of (a) P25, (b) TiO_2 , nanoparticles and (c) $\text{TiO}_2\text{:Ag}$ nanoparticles.

intense narrow absorption peak at 360 nm (Figure 4c) is red shifted compare to TiO_2 nanomaterials. It clearly indicates that Ag nanoparticles were successfully associated with TiO_2 nanoparticles. This red shift indicates that TiO_2 :Ag nanoparticles have much stronger absorption than that of TiO_2 nanoparticles, i.e., TiO_2 :Ag nanoparticles possess higher photocatalytic activity than undoped TiO_2 nanoparticles²⁷.

TGA analysis was employed to determine the thermal stability of the as-prepared materials. **Fig.5** shows the TGA of as-prepared TiO_2 :Ag nanoparticles at 120 °C for 1 day via ionic liquid assisted hydrothermal method. There are two weight loss stages were observed. The weight loss from room temperature to 100 °C is due to the presence of adsorbed water molecules. The second weight loss from 100 °C to 400 °C can be attributed to thermal decomposition of organic substances (ionic liquids)²⁸. Above 400 °C almost there is no weight loss occurred indicates that TiO_2 :Ag nanoparticles are thermally stable upto 700 °C.

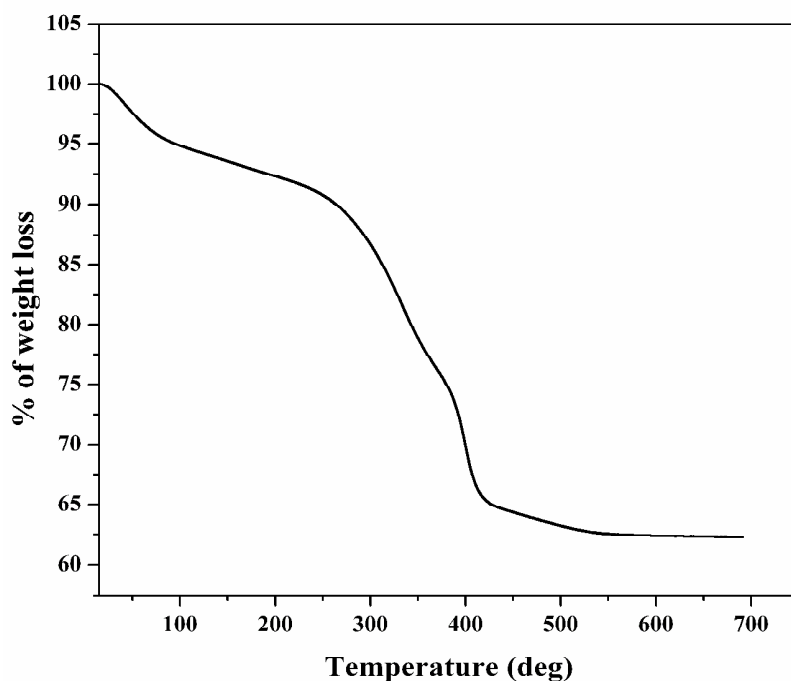


Figure 5. Thermo gravimetric analysis of TiO_2 :Ag nanoparticles

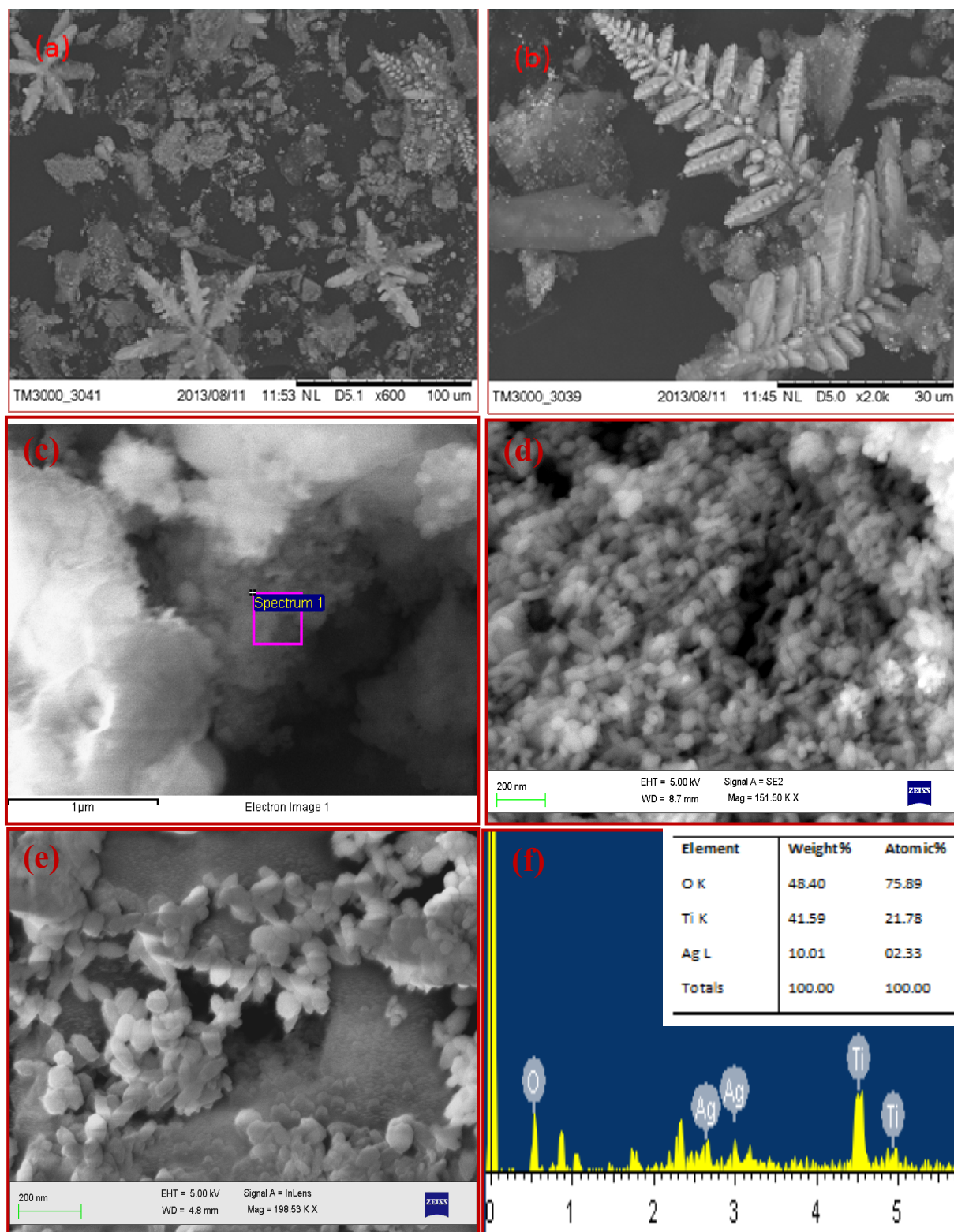


Figure 6. SEM images and EDS spectrum of $\text{TiO}_2:\text{Ag}$ nanoparticles

Amount of silver leached/discharged from the $\text{TiO}_2:\text{Ag}$ photocatalyst was estimated using direct air-acetylene flame method. In case of 0.1 g of $\text{TiO}_2:\text{Ag}$ in 100 mL water, amount of doped silver discharged from photocatalyst ($\text{TiO}_2:\text{Ag}$ nanomaterial) was found to be $0.26 \mu\text{g/L}$, for 0.2 g of photocatalyst in 100 mL water, amount of silver discharged from photocatalyst was $0.33 \mu\text{g/L}$, for 0.3 g of $\text{TiO}_2:\text{Ag}$ nanomaterial in 100 mL water was $0.37 \mu\text{g/L}$. **Fig.6(a),(b)** shows the SEM images of $\text{TiO}_2:\text{Ag}$ nanoparticles prepared via ionic liquid assisted hydrothermal method and are closely resemble fern-like phyllotaxy. i.e. shows hyper branched structure, grows with pronounced trunks with $100 \mu\text{m}$ and $30 \mu\text{m}$ dimensions respectively. $\text{TiO}_2:\text{Ag}$ nanoparticles which have corrugations and ordered branches that are symmetrically distributed on opposite sides of the trunks. Low magnification SEM image (**Fig.6(c)**) shows that the $\text{TiO}_2:\text{Ag}$ nanoparticles are agglomerated to form a cloud like morphology. High magnified SEM images (**Fig.6 (d), (e)**) clearly shows the presence of nanoparticles. EDS spectrum is mainly used to identify the elements present in the prepared materials and Fig. 6f clearly shows the presence of Ti, O and Ag.

Fig.7 shows the TEM images of $\text{TiO}_2:\text{Ag}$ nanoparticles prepared at 120°C for 1 day are looking like almost rice shape and the size of the nanoparticles was found to be $\sim 60 \text{ nm}$. Due to the large atomic radius of the silver atom, they cannot interpenetrate in TiO_2 crystal lattice to form solid solution alloy. Therefore, Ag nanoparticles distributes in TiO_2 matrix. In general the TiO_2 particles appear transparent. Dark region indicated by arrow clearly indicates the presence of almost spherical shaped Ag nanoparticles²⁹⁻³⁰.

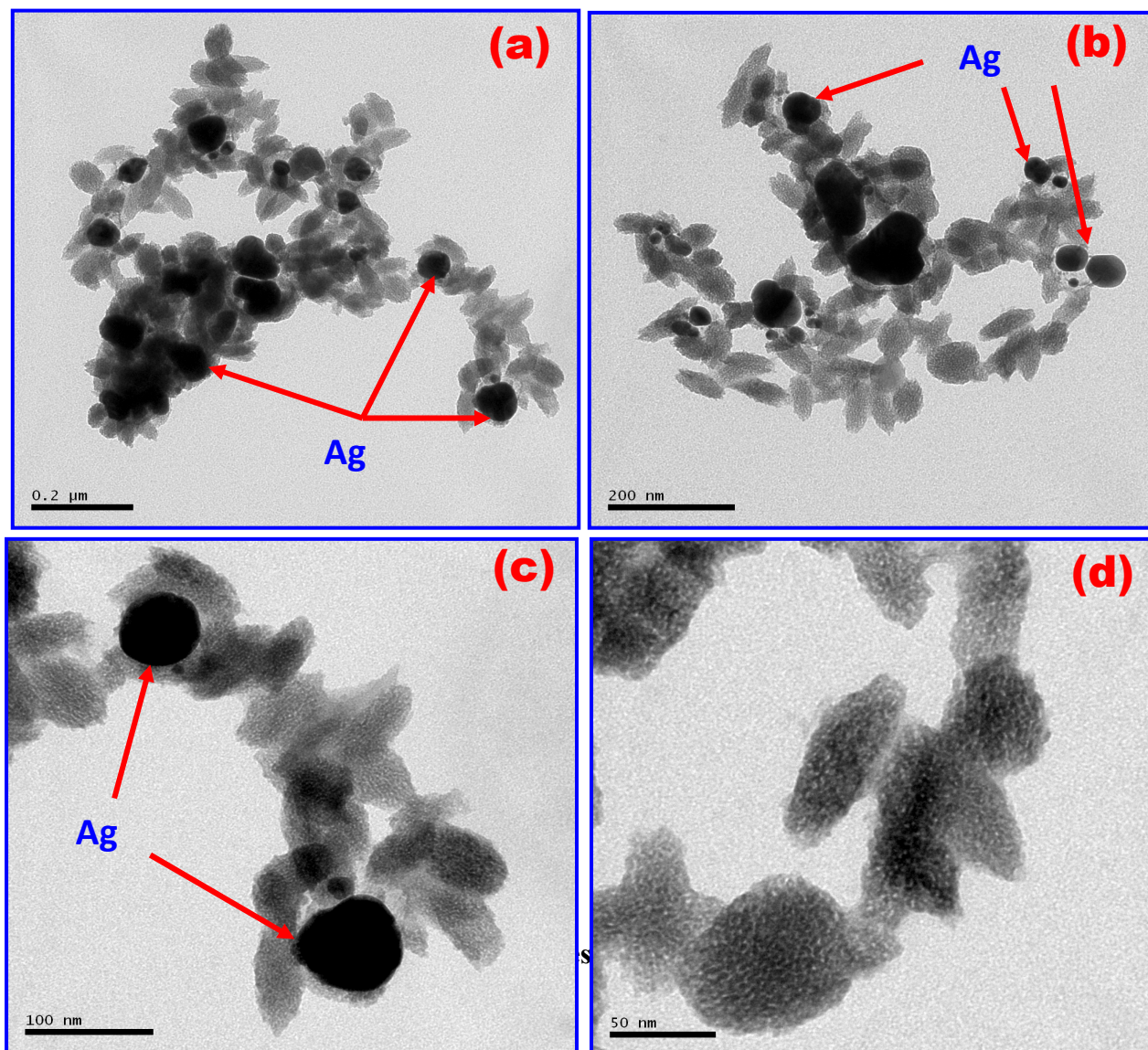


Figure 7. TEM images of $\text{TiO}_2:\text{Ag}$ nanoparticles.

3.2. Hydrogen generation

Fig.8. shows the hydrogen generation of P25, TiO_2 nanoparticles, $\text{TiO}_2:\text{Ag}$ nanoparticles and only water ethanol system in absence of the catalyst. Liu et al. reported that Ag deposited TiO_2 nano-sheet film showed 8.5 times higher photocatalytic water splitting for hydrogen generation than the bare TiO_2 nanomaterials²⁹. From the graph it is cleared that $\text{TiO}_2:\text{Ag}$ nanoparticles liberates 2230 $\mu\text{mol H}_2$ generated per 1 g of photocatalyst at 2.5 h compare to bare TiO_2

nanoparticles (1200 $\mu\text{mol H}_2$ generated per 1 g of photocatalyst at 2.5 h) and P25 (707 $\mu\text{mol H}_2$ generated per 1 g of photocatalyst at 2.5 h). Controlled experiment clearly suggests that the liberation of H_2 is due to the presence of catalyst.

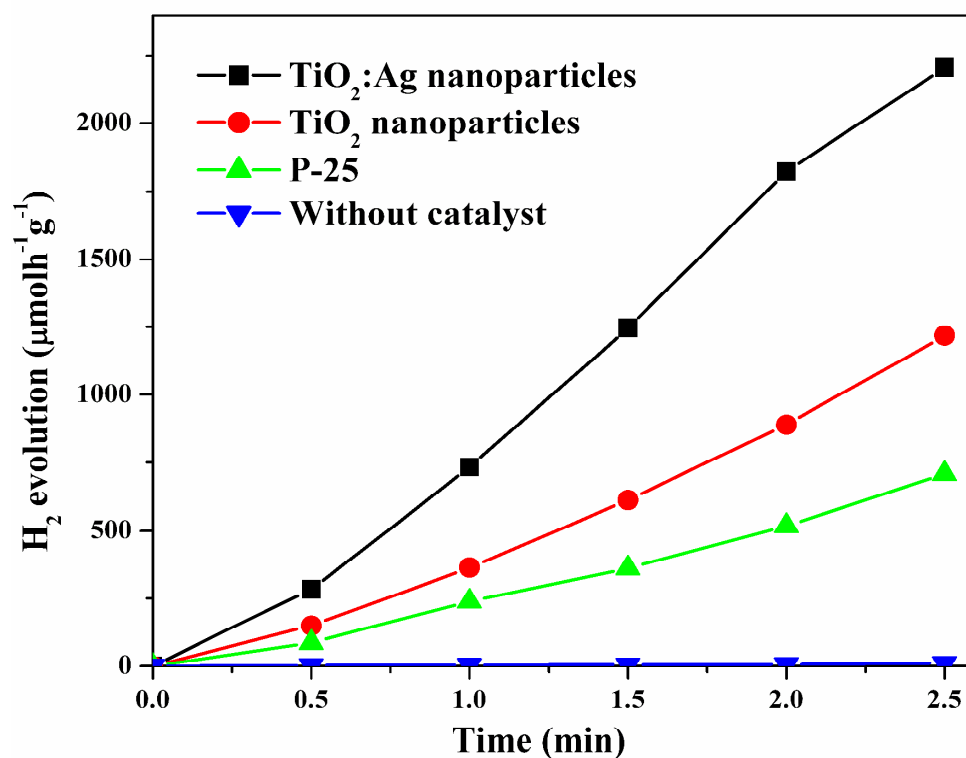


Figure 8. Hydrogen generation of (a) P-25 (b) TiO_2 and (c) TiO_2 :Ag nanoparticles

3.3. Photocatalytic degradation of trypan blue

3.3.1. Effect of dye concentration

Effect of dye concentration on the photocatalytic activity TiO_2 : Ag nanoparticles prepared at 120 °C for 1 day by ionothermal method as shown in **Fig.9**. Concentration of trypan blue was varied from 5 to 25 $\mu\text{g/L}$ and catalytic load was maintained at 400 mg at pH 8. As the concentration of dye increases, time taken for the complete degradation also increases. At higher concentration

more dye molecules are adsorbed on to the surface of catalyst resulting in decreased active sites on the catalyst (lesser number of hydroxyl and superoxide radicals) and thereby, reduced the light penetration.

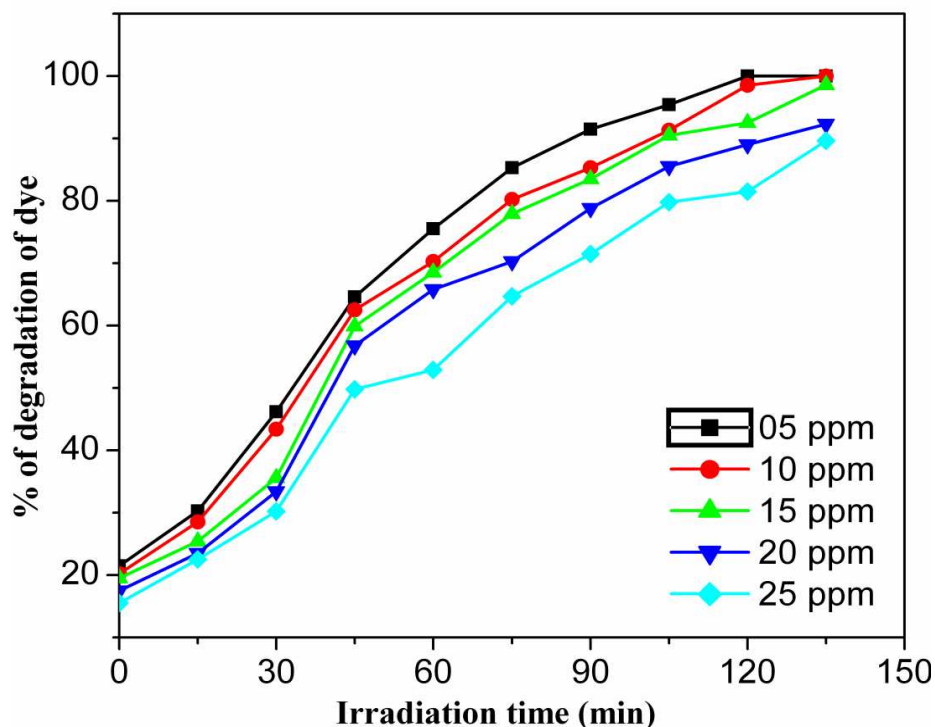


Figure 9. Effect of dye concentration on the photocatalytic activity.

3.3.2. Effect of catalyst dosage

Effect of catalyst load on the photocatalytic degradation of dye is as shown in **Fig.10**. In order to determine the optimal dosage of the catalyst; the catalytic load was varied from 100-500 mg/100 mL. The optimal load was found to be 400 mg/100 mL. Above the optimal load, turbidity of the solution increases, light penetration decreases and thus availability of hydroxides and super oxides becomes minimal.

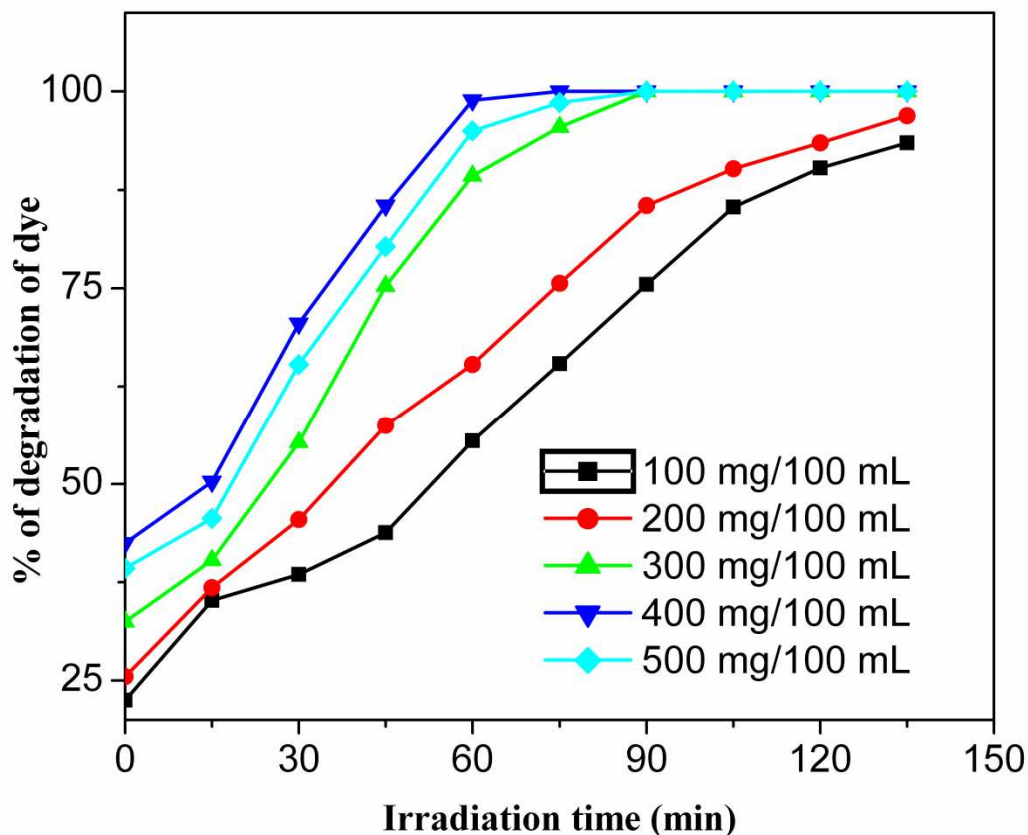


Figure 10. Effect of catalytic load on the photocatalytic activity

3.3.3. Effect of pH on photocatalytic degradation

Fig.11. shows the effect of pH on photocatalytic degradation of trypan blue. From the figure it is clear that photocatalytic process is strongly depends on the pH of the dye solution³¹. The pH of the solution is adjusted by the addition of either 0.1 M NaOH or 0.1 M H₂SO₄. The degradation efficiency is more in basic medium than in acidic. This observation matches well with the reported studies³². The variation of pH alters the surface properties of TiO₂: Ag nanoparticles, in turn dissociation of the dye molecules. At pH 8, perhydroxyl radicals are formed, leading to the formation of hydrogen peroxide which gives more number of hydroxyl radicals. The highest photocatalytic degradation is observed at pH 8 and this is in good agreement with literature³³.

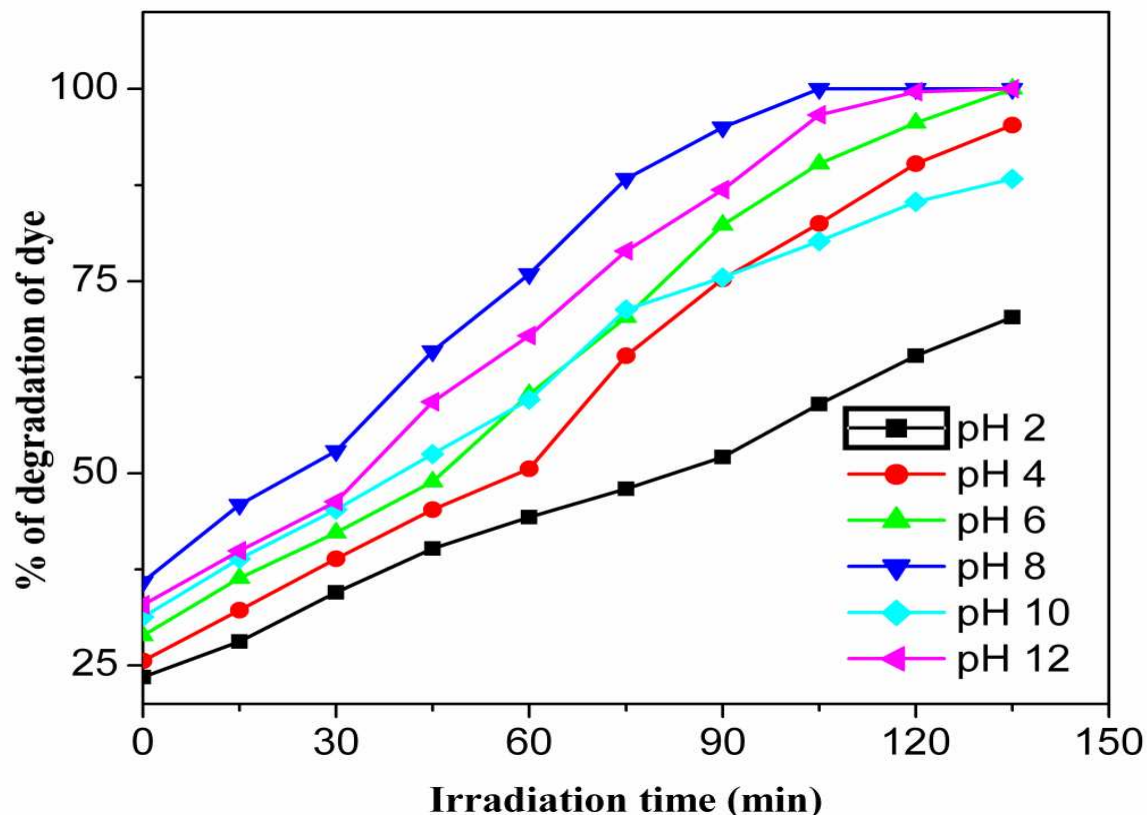


Figure 11. Effect of pH on photocatalytic degradation of trypan blue

3.3.4. Effect of different nature of light source on photocatalytic activity

Fig.12. shows the effect of different light source on photocatalytic degradation. Two different light sources are used namely sun light and UV light. From the figure, it is clear that photocatalytic degradation of the dye was more in UV light than in sun light. This is due to the fact that UV light has higher intensity (lower wavelength or higher energy), hence light can easily penetrate and result in the formation of more number of radicals, which increases the rate of photocatalytic degradation of an azo dye.

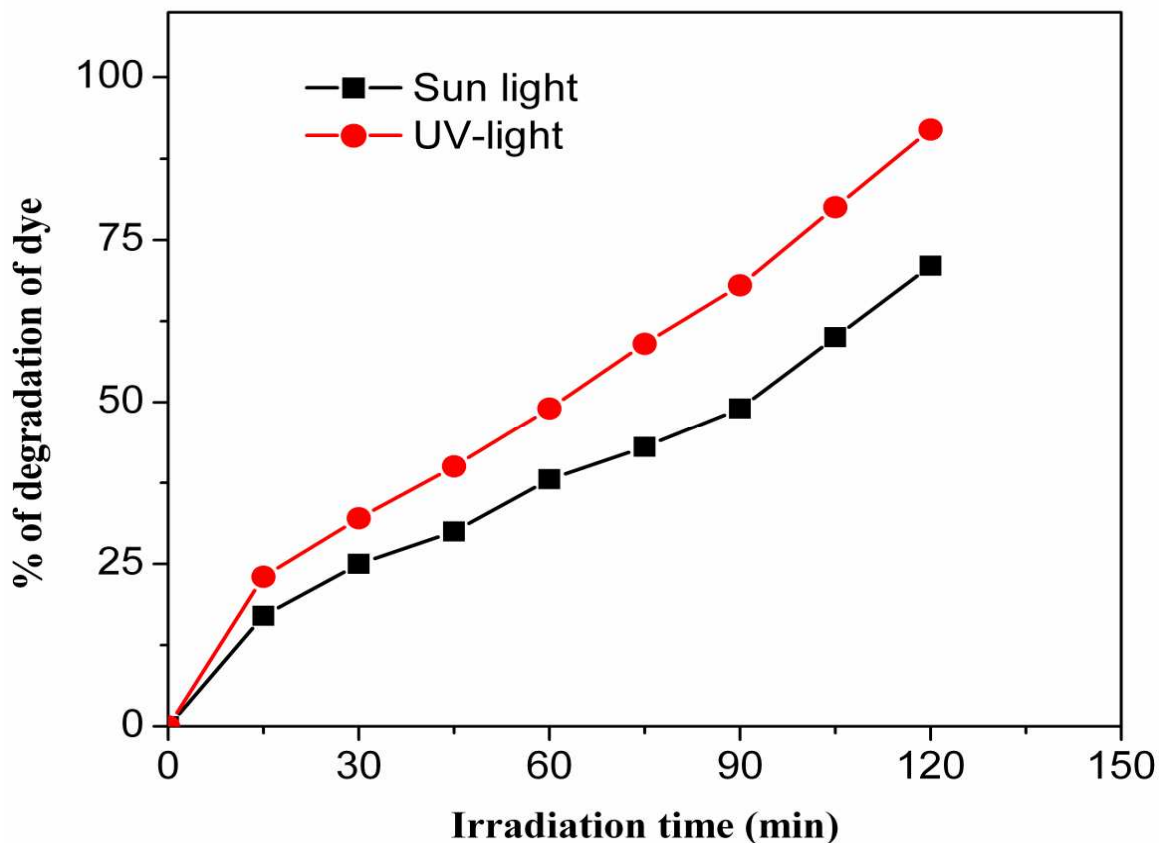


Figure12. Effect of different light source on photocatalytic degradation

3.3.5. Effect of recyclability of $\text{TiO}_2\text{:Ag}$ nanoparticles on photocatalytic degradation

Fig.13. shows the effect of recyclability of $\text{TiO}_2\text{:Ag}$ nanoparticles prepared at $120\text{ }^\circ\text{C}$ for 1 day by ionothermal method on photocatalytic degradation of trypan blue. One of the today's main industrial wastewater treatment strategies is focused on the development of green technologies. $\text{TiO}_2\text{:Ag}$ nanoparticles recycling can be foreseen as a good practice for sustainable industrial waste treatment. Consequently, it is necessary to demonstrate whether, after a photocatalytic treatment, the catalyst can be reused. The nanoparticles were used and recycled for consecutively

three times. Photocatalytic reaction was carried out at constant dye concentration (10 $\mu\text{g/L}$) and constant catalytic load (400 mg/100 mL of trypan blue). Once the first set of experiment is completed, the catalyst is retrieved from the solution by centrifugation and dried in an oven. The recycled catalyst was used for the second cycle and so on. These experimental studies indicated that the rate of photo degradation activity of $\text{TiO}_2\text{:Ag}$ was decreases as the number of cycle increases. This could be due to the aggregation and sedimentation of the dye around $\text{TiO}_2\text{:Ag}$ after each cycle of photocatalytic degradation. Each time, the catalyst is reused new parts of the catalyst surface become unavailable for dye adsorption and thus photon absorption, reducing the efficiency of the catalytic reaction³⁴.

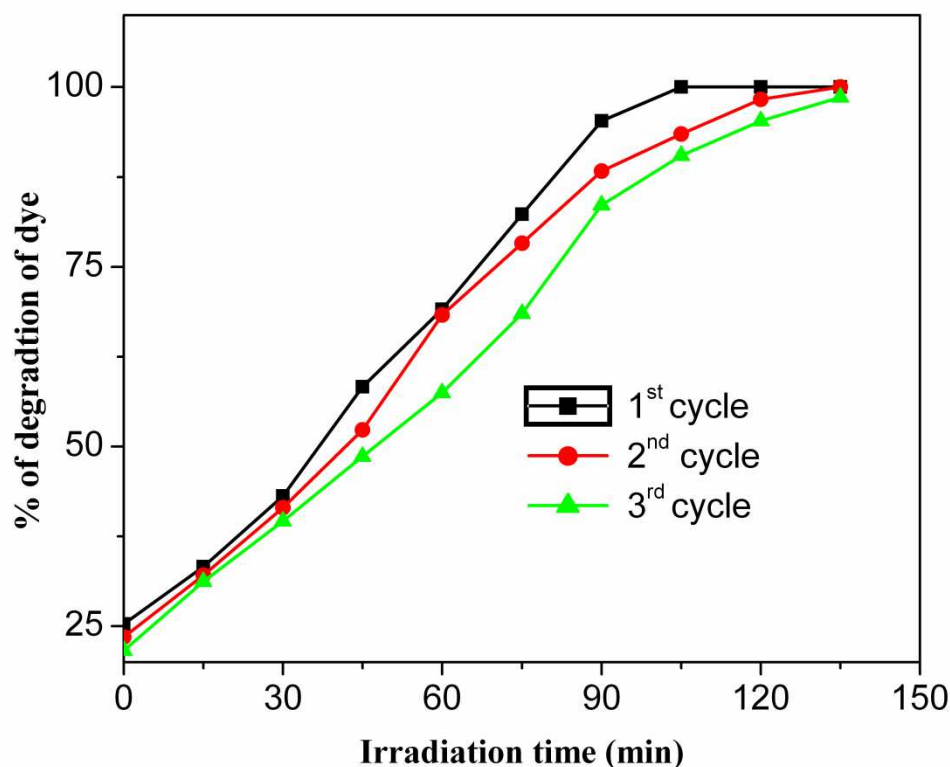


Figure13. Effect of recyclability of $\text{TiO}_2\text{:Ag}$ nanoparticles on photocatalytic degradation.

4. Conclusions

We have successfully synthesized TiO₂:Ag nanoparticles via ionic liquid assisted hydrothermal method using imidazolium based functionalized ionic liquid at 120 °C for one day. XRD and XPS indicated the presence of Ag nanoparticles on anatase TiO₂ nanoparticles. EDS also clearly shows the presence of Ag, in addition to Ti and O. FTIR spectrum indicates the presence of Ag-O in addition to Ti-O vibration modes. UV-Vis spectrum of TiO₂:Ag nanoparticles shows a band gap of 3.41 eV which is red shifted compare to TiO₂ nanoparticles. SEM images resembles to leaf-like structure. TEM images clearly show the presence of Ag in the composite evidenced by dark region and the size of the nanoparticle is found to be ~ 60 nm. TGA shows the presence of ionic liquids observed by the weight loss up-to 400 °C. TiO₂:Ag nanoparticles shows enhanced H₂ generation (2230 μmol H₂ generated per 1 g of photocatalyst per 1 h) compare to bare TiO₂ (1200 μmol H₂ generated per 1 g of photocatalyst per 1 h) and P 25 (707 μmol H₂ generated per 1 g of photocatalyst per 1 h) indicates that these nanoparticles are promising candidate for photocatalytic H₂ generation via water splitting reaction. It also shows good enhanced photocatalytic activity for the degradation of toxic azo dye-trypan blue compare to bare TiO₂ nanoparticles.

Acknowledgement: One of the authors, T.N. Ravishankar wishes to acknowledge Jain University, for support and funding to carry out the research work.

References

- 1 X. Chen and S. S. Mao, *Chem. Rev*, 2007, **107**, 2891.
- 2 A.M. Morales and C.M. Lieber, *Science*, 1998,**279**, 208.
- 3 J. Gopalakrishnan, *Chem. of Mater*, 1995, **7**, 1265.
- 4 L. Brennan and P. Owende, *Renew and Sus. Ener. Rev*, 2010, **2**, 557.
- 5 J. Wang and W. Wan, *Int. J. Hydro. Ener*, 2009, **34**,799.
- 6 G. Nagaraju, T.N. Ravishankar, K. Manjunatha, S. Sarkar, H. Nagabhushana, R. Goncalves and J. Dupont, *Mat. Lett*, 2013,**109**, 27.
- 7 K. Hashimoto, H. Irie and A. Fujishima, *Jap. J. Appl. Phys*, 2005, **44**, 8269.
- 8 X. Li, Q. Liu, X. Y. Jiang and J. Huang, *Int. J. Electrochem. Sci*, 2012, **7**, 11519.
- 9 P.R. Mishra and O.N. Shrivastava, *Bull. Mater. Sci*, 2008, **31**, 545.
- 10 G. Singh and A. Kumar, *Ind. J. Chem*, 2008, **47A**, 495.
- 11 A. Zaleska , *Rec. Patents on Eng*, 2008, **2**, 157.
- 12 B. Cheng, Y. Le and J. Yu, *J. Hazardous. Mater*,2010, **117**, 971.
- 13 K. Zhou, Y. Zhu, X. Yang, X. Jiang and C. Li, *New J. Chem*, 2011, **35**, 353.
- 14 M. Logar, B. Jancar, S. Sturm and D. Suvorov, *Langmuir*, 2010, **26**, 12215.
- 15 M.C. Hidalgo, M. Maicu, J.A. Navio and G. Colon, *Catal. Today*, 2007, **129**, 43.
- 16 P. Kormali, A. Troupis, T. Triantis, A. Hiskia and E. Papaconstantinou, *Catal.Today*, 2007, **124**,149.
- 17 M. Ni, M.K.H. Leung, D.Y.C. Leung and K. Sumathy, *Renew and Sus. Ener. Rev*, 2007, **11**, 401.
- 18 Y.R. Jin, Y.H. Jung, S.J. Park and I.H. Baek, *Korean .Chem. Eng. Res*,2012, **1**, 35.
- 19 S.S. Mandal and A. J. Bhattacharyya, *J. Chem, Sci*, 2012,**124**, 969.
- 20 J.F. Weaver and G.B. Hoflund, *J. Phys. Chem*, 1994, **98**, 8519.

- 21 Y.Q. Liang, Z.D. Cui, S.L. Zhu, Y. Liu and X.J. Yang, *J. Catalysis*, 2011, **278**, 276.
- 22 R. Wahab, S.G. Ansari, K. Seo and G.S. Kim, *Mater. Res. Bull.* 2007, **42**, 1640.
- 23 T.K. Gupta and P.L. Hower, *J. Appl. Phys.*, 1992, **50**, 4849.
- 24 K. Johannes, F. Juergen and L. Alfred, *Appl. Spec.*, 2007, **61**, 1306.
- 25 G. Nagaraju, K. Manjunath, T.N. Ravishankar. B.S. Ravikumar, H. Nagabhushan, G. Ebeling and J. Dupont, *J. Mater. Sci.* 2013, **48**, 8420.
- 26 Y. Lai, H. Zhang, K. Xie, D. Gong and Z. Chen, *New. J. Chem.* 2010, **34**, 1335.
- 27 G. Kiran, R.P. Singh, A. Pandey and P. Anjana , *Beilstein J. Nanotechol.* 2013, 4, 345.
- 28 Q. Zhang, Y.Q. He, X.G. Chen, D.H. Hu, L.J. Li, T. Yin, L.L. Ji, *Chin. Sci. Bull*, 2011, **56**, 331.
- 29 E. Liu, L. Kang, Y. Yang, T. Sun, X. Hu, C. Zhu, H. Liu, Q. Wang, X. Li and J. Fan, *Nanotechnology*, 2014, **25**, 165401.
- 30 T.D. Pham and B.K. Lee, *Int. J. Environ. Res. Publ. Health*, 2014, **11**, 3271.
- 31 W. Smith, S. Mao, G. Lu, A. Catlett, J. Chen and Y. Zhao, *Chem. Phys. Lett.* 2010, **485**, 171.
- 32 A. Khanna and K.V. Shetty, *Environ. Sci. Pollut. Res. Int.*, 2013, **20**, 5692.
- 33 N. Hariprasad, S.G. Anju , E.P. Yesodharan and Y. Suguna, *Res. J. Material. Sci*, 2013, **1**, 9.
- 34 H. Trabelsi, P. Atheba, G. K. Gbassi, M. Ksibi, P. Drogui, *Int. J. of Hazard Mater*, 2012, **1**, 6.